Review Article

Biomedical application of terahertz imaging technology: a narrative review

Mengyang Cong[1], Wen Li[2], Yang Liu[2], Jing Bi[2], Xiaokun Wang[2], Xueqiao Yang[2], Zihan Zhang[2], Xiaoxin Zhang[2], Ya-Nan Zhao[2], Rui Zhao[2,3,4], Jianfeng Qiu[2,5]

[1]College of Mechanical and Electronic Engineering, Shandong Agricultural University, Tai'an, China; [2]School of Radiology, Shandong First Medical University & Shandong Academy of Medical Sciences, Tai'an, China; [3]Department of Nuclear Medicine, The First Affiliated Hospital of Shandong First Medical University & Shandong Provincial Qianfoshan Hospital, Jinan, China; [4]Science and Technology Innovation Center, Shandong First Medical University & Shandong Academy of Medical Sciences, Jinan, China; [5]Center for Medical Engineer Technology Research, Shandong First Medical University & Shandong Academy of Medical Sciences, Tai'an, China

Contributions: (I) Conception and design: M Cong, R Zhao, J Qiu; (II) Administrative support: J Qiu, R Zhao; (III) Provision of study materials or patients: All authors; (IV) Collection and assembly of data: W Li, Y Liu, J Bi, X Wang, X Yang, Z Zhang, X Zhang, YN Zhao; (V) Data analysis and interpretation: M Cong; (VI) Manuscript writing: All authors; (VII) Final approval of manuscript: All authors.

Correspondence to: Jianfeng Qiu, PhD. School of Radiology, Shandong First Medical University & Shandong Academy of Medical Sciences, Tai'an, China; Center for Medical Engineer Technology Research, Shandong First Medical University & Shandong Academy of Medical Sciences, Changcheng Road, Tai'an 271016, China. Email: jfqiu100@gmail.com; Rui Zhao, PhD. School of Radiology, Shandong First Medical University & Shandong Academy of Medical Sciences, Tai'an, China; Science and Technology Innovation Center, Shandong First Medical University & Shandong Academy of Medical Sciences, Jinan, China; Department of Nuclear Medicine, The First Affiliated Hospital of Shandong First Medical University & Shandong Provincial Qianfoshan Hospital, Jingshi Road, Jinan 250000, China. Email: zhaorui@sdfmu.edu.cn.

Background and Objective: Terahertz (THz) imaging has wide applications in biomedical research due to its properties, such as non-ionizing, non-invasive and distinctive spectral fingerprints. Over the past 6 years, the application of THz imaging in tumor tissue has made encouraging progress. However, due to the strong absorption of THz by water, the large size, high cost, and low sensitivity of THz devices, it is still difficult to be widely used in clinical practice. This paper provides ideas for researchers and promotes the development of THz imaging in clinical research.

Methods: The literature search was conducted in the Web of Science and PubMed databases using the keywords "Terahertz imaging", "Breast", "Brain", "Skin" and "Cancer". A total of 94 English language articles from 1 January, 2017 to 30 December, 2022 were reviewed.

Key Content and Findings: In this review, we briefly introduced the recent advances in THz near-field imaging, single-pixel imaging and real-time imaging, the applications of THz imaging for detecting breast, brain and skin tissues in the last 6 years were reviewed, and the advantages and existing challenges were identified. It is necessary to combine machine learning and metamaterials to develop real-time THz devices with small size, low cost and high sensitivity that can be widely used in clinical practice. More powerful THz detectors can be developed by combining graphene, designing structures and other methods to improve the sensitivity of the devices and obtain more accurate information. Establishing a THz database is one of the important methods to improve the repeatability and accuracy of imaging results.

Conclusions: THz technology is an effective method for tumor imaging. We believe that with the joint efforts of researchers and clinicians, accurate, real-time, and safe THz imaging will be widely applied in clinical practice in the future.

Keywords: Terahertz (THz) image; breast; brain; skin; cancer

Submitted Apr 17, 2023. Accepted for publication Aug 31, 2023. Published online Sep 27, 2023.
doi: 10.21037/qims-23-526
View this article at: https://dx.doi.org/10.21037/qims-23-526

Introduction

Terahertz (THz) wave refers to electromagnetic radiation with a frequency of 0.1–10 THz (a wavelength of 30–3,000 μm), which is between the microwave and infrared regions. Compared to other bands, the THz wave has good penetration properties for many non-polar and non-metallic substances. At the same time, THz waves are strongly absorbed by water molecules. THz radiation is non-ionizing and non-invasive due to its very low photon energy. Many organic molecules have strong absorption and scattering characteristics for the THz spectrum due to low-frequency vibration and rotational transitions of the molecules, so that each molecule has its own unique "fingerprint spectrum" (1-3). As a result, the THz technology has been applied in the field of food (4,5), agriculture (6,7), biology (8-10), security inspection (11) and communications (12,13).

THz technologies are mainly divided into THz spectroscopy and THz imaging technology. THz spectrometers are mainly divided into three categories: Fourier transform spectroscopy (FTS), photo-mixing spectrometer and THz time-domain spectroscopy (THz-TDS) (14). Although FTS has a poor signal-to-noise ratio (SNR), it has a wide spectral coverage (100 GHz–5 THz). Due to the high spectral density and high frequency resolution, the photomixing spectrometer is a highly accurate and simple instrument, but its measurement takes a long time. THz-TDS is the Fourier transform of the THz time domain signal of the sample into absorption coefficient, refractive index (RI) and transmittance. This technology provides a time-resolved spectral analysis, and effectively suppresses some common sources of noise. The basic principle of the THz imaging system is as follows: place the sample on the XYZ platform to change its position; then collect and process information of the THz wave (amplitude and/or phase) at different positions of the sample; finally, construct a point-by-point image. THz imaging is mainly divided into THz pulse imaging (TPI) systems and continuous wave (CW) THz imaging systems. TPI is generated by a femtosecond pulsed laser. Although it requires a longer scanning time, the intensity and phase information of the THz waveform can be recorded to obtain more details of the sample (15). The CW imaging system is generated by a CW laser. It is of small size and low cost, but its application range is limited due to the narrow source spectrum.

There are currently many problems to be solved with THz technology. The high-power and high-efficiency THz radiation source is the main challenge that researchers need to overcome. Two researches have shown that spintronic-based and intense laser-driven THz sources can achieve higher output power (16,17). It is also crucial to achieve a THz device with high sensitivity, ultra compactness, and broadband detection. Quantum sensing technology and metamaterials are being applied to THz detectors to solve the above problems (18,19). The problem of high cost and large volume of THz devices can be solved by solid-state electronic oscillators.

This review has mainly summarised the development of THz imaging technology in biomedical applications. At present, biomedical imaging technology mainly includes X-ray, computed tomography (CT), magnetic resonance imaging (MRI) and so on. Compared with X-ray and CT, THz technology has almost no radiation hazard to the human body and significantly improves the sensitivity of tumors differentiation in a non-ionizing way (20). Compared with MRI, THz technology has a suitable penetration depth for superficial tumors. And small handheld devices for intraoperative imaging can be developed using this technology (8). THz medical imaging is based on differences of water content in tissue and structural changes: cancer tissue contains more water due to tissue edema and increased cellularity, resulting in different THz absorption; pathological changes in the tissue lead to changes in the microenvironment and cellular structure, resulting in differences in imaging (8,21). According to the basic mechanism of THz medical imaging, this technology has been applied to breast, brain, skin, liver, colon cancer, diabetic foot, bone, cervical cancer, etc. (22-29).

The content of this paper is mainly divided into the following aspects: various THz medical imaging techniques were introduced in section 2; in sections 3, 4 and 5, we mainly discussed the research progress of THz imaging technology in breast, brain and skin tissues in the past six years; finally, some suggestions for the future development of THz medical imaging were put forward. We present this

Table 1 The search strategy summary

Items	Specification
Date of search	17/02/2022–01/10/2022
Databases and other sources searched	Web of Science and PubMed
Search terms used	"Terahertz imaging", "Terahertz imaging" + "Breast", "Terahertz imaging" + "Brain", "Terahertz imaging" + "Skin" and "Terahertz imaging" + "Cancer"
Timeframe	2017–2022
Inclusion and exclusion criteria	Published full-text journals and conference papers in English, excluding reviews and non-English papers. Papers that utilized terahertz imaging for biological tissue imaging were selected, otherwise excluded
Selection process	The literature selection was done independently by Cong M. Differences were resolved by consensus

article in accordance with the Narrative Review reporting checklist (available at https://qims.amegroups.com/article/view/10.21037/qims-23-526/rc).

Methods

A comprehensive search was conducted in the Web of Science and PubMed databases to review existing research on the THz imaging technology and cancer. We searched for the following keywords: "Terahertz imaging", "Breast", "Brain", "Skin" and "Cancer". The search time range was from January 1, 2017 to December 30, 2022. The search strategy summary is shown in *Table 1*.

THz imaging technique

THz near-field imaging

In the THz range, the spatial resolution of the traditional far-field spectrum is limited by the diffraction limit, which is about half the wavelength, leading to imaging limitations. To improve the spatial resolution, the near-field THz wave can be generated by using the metal tip and small aperture (30,31). In addition, placing the sample close to the detector is the simplest method to achieve the near-field THz electric field (32). The near-field scanning imaging system based on the conventional THz optical waveguide antenna uses the unbiased antenna and microprobe as the THz transmitter and detector, respectively. Through the coupling between the probe tip and the near-field, the probe can be placed close to the sample surface. Geng *et al.* modified the traditional THz near-field imaging system based on a photoconductive antenna microprobe (PCAM) (33). They used a delay line based on a voice coil motor, which increased the imaging speed by 100 times. The probe-sample separation range could be controlled within a few microns to meet the requirements of THz near-field imaging of biological samples. Li *et al.* developed a PCAM-based near-field THz-TDS system (*Figure 1A*) (34). The spatial resolution of the system had reached 3 μm, which was 1–2 orders of magnitude higher than the traditional THz imaging system. The changes in cell morphology during natural drying were successfully monitored (*Figure 1B*).

In addition to the technologies mentioned above, the THz scattering type scanning near-field optical microscope (THz s-SNOM) based on the atomic force microscope (AFM) using metal or metal-coated tips is also a very powerful near-field imaging technology (37). It had been demonstrated that this technology can provide nanometer spatial resolution. Nevertheless, due to the weak THz scattering properties of biomolecules, THz nanoimaging of single biomolecules remains unsolved. Yang *et al.* used a graphene substrate with high THz reflectivity and atomic flatness to minimize the topographic noise. At the same time, the free propagation of the THz electric field was concentrated in the vicinity of the platinum (Pt) probe. In order to enhance the THz near-field signal and ensure mechanical stability, the Pt probe with a shaft length of 100 μm was selected for the experiment. This study ultimately provided the morphology and THz scattering images of single biomolecules at the nanometer scale (38).

THz single-pixel imaging

The traditional THz-TDS imaging system requires raster scanning pixel-by-pixel to reconstruct the THz

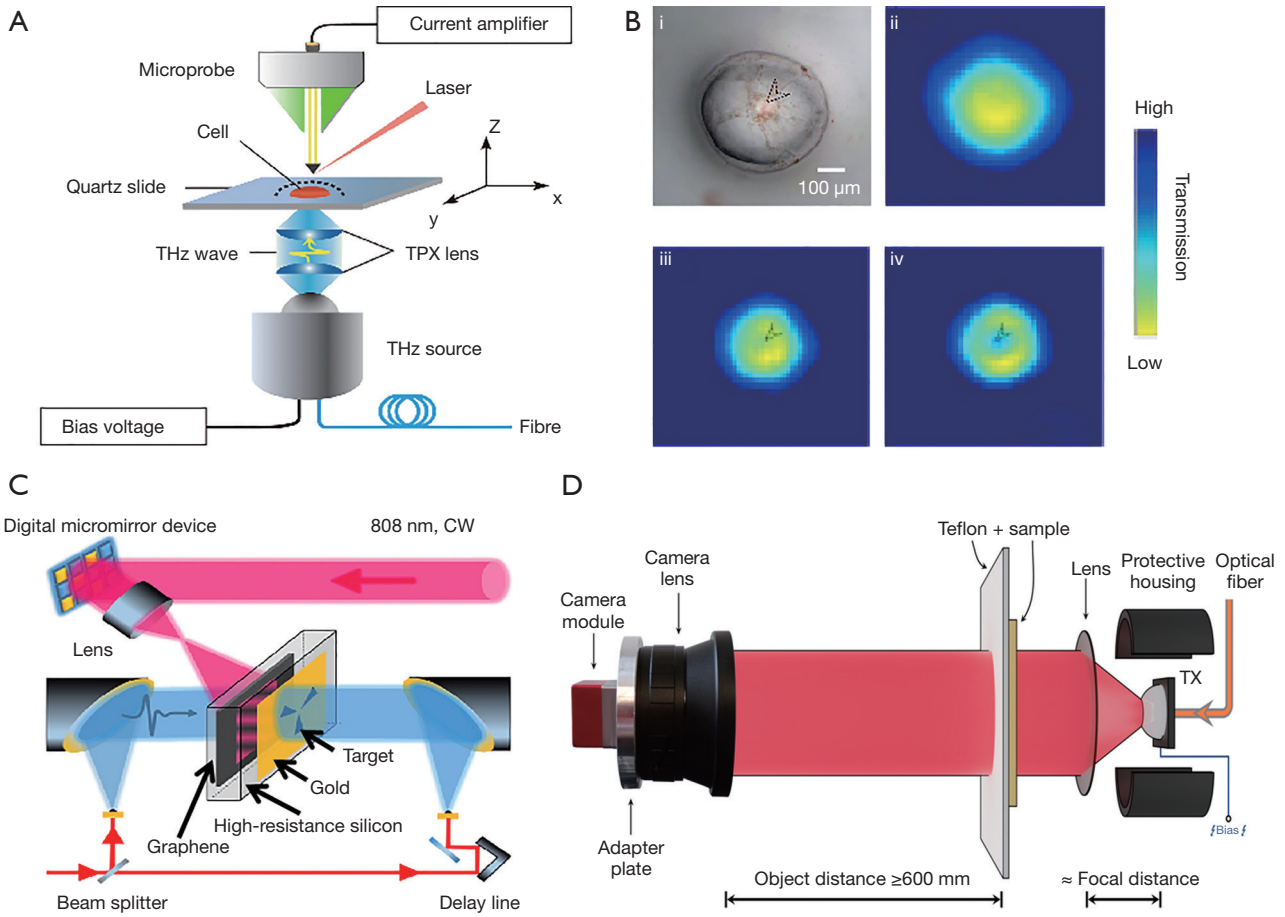

Figure 1 Schematic diagram of the THz device. (A) Schematic illustration of the experimental setup (34). (B) Changes in cell morphology during natural drying: (i) optical image; (ii-iv) THz image of cells dried for 1, 3, 5 h (34). (C) Schematic of THz single pixel imaging. A spatial modulator is made by combining graphene, silicon and gold to improve image quality (35). (D) Schematic of the imaging setup. Remove all OAPMs and illuminate the sample directly. Images were captured using a lens designed specifically for RIGI cameras (36). TPX, methyl pentene copolymer; THz, terahertz; CW, continuous wave; TX, transmitter; OAPMs, off-axis parabolic mirrors.

time waveform, which greatly increases the acquisition time. Single-pixel imaging technology uses modulation technology to encode the spatial information of the THz wave, and it uses a single-point detector to collect the reflected light or transmitted light after the spatially encoded THz wave irradiates the target information. Finally, the two-dimensional image of the target is reconstructed by a decoding algorithm (39,40).

The core components of single pixel imaging are spatial light modulators (SLMs) and reconstruction algorithms. The compressed sensing (CS) imaging algorithm is one of the most commonly used reconstruction algorithms (41). This algorithm essentially consists of compressed sampling and computational image reconstruction. The compressed signal is transformed into a high-dimensional signal that is projected onto a low-dimensional space. A reconstruction algorithm is used to solve an optimization problem. Ultimately, the original signal can be reconstructed with high probability from these few projections. The algorithm reconstructs high-quality THz images by measuring fewer pixels (42). At the same time, the combination of CS and inverse Fresnel diffraction (IFD) algorithms has reconstructed clear THz single-pixel images (43). THz imaging is limited by the diffraction limit, resulting in low resolution and unable to meet the requirements of high-precision measurement. The IFD algorithm can effectively eliminate the diffraction effects in THz fields, thus greatly improving the resolution of THz imaging. She *et al.*

proposed a new THz single-pixel imaging technology based on the spatial Fourier spectrum (*Figure 1C*) (35). Graphene was added to the traditional THz modulator to reconstruct the THz image. CS imaging is difficult to achieve real-time imaging. In this study, a partially sampled Adama matrix and a regularized image reconstruction matrix were employed to reduce the computation time, and achieved 32×32 resolution at a speed of about 6 frames per second (44). Moreover, to get insight into hidden objects, the single-pixel imaging technology could be used to achieve two-dimensional tomographic THz imaging (45). Recently, Li *et al.* designed a SLM based on tunable liquid crystals (LCs) for THz single-pixel compressive imaging. The proposed frequency switching method based on LC-SLM and auto-calibrated compressive sensing (ACCS) algorithm can improve the frame rate limit, saving almost half of the imaging time (46). The use of frequency selective SLM for single-pixel imaging based on LC, micro electromechanical systems (MEMS), and phase change materials has great potential. It provides a reliable and low-cost method.

THz real-time imaging

With the development of highly sensitivity and real-time THz detectors, real-time THz imaging has been widely used in security and medical fields (47,48). The most common real-time THz imaging technologies are fast optical delay lines, photoconductive antenna arrays, and electro-optical camera sampling (49). Traditional THz imaging systems used raster scanning, which took a long time to acquire image data. A broadband THz spectral imaging system with a highly sensitive THz camera was used for real-time imaging (50). Usually, the thermal detector achieved real-time imaging by using the focal plane array, but it had the disadvantage of low sensitivity. To overcome this shortcoming, a new optomechanical element molecular array was invented, which successfully obtained THz images of metal and biological objects in real time (51). Perraud *et al.* achieved real-time three-dimensional imaging by focusing on the shape algorithm (52). Zolliker *et al.* combined a commercial fiber-coupled photoconductive antenna THz source with a microbolometer camera to propose a real-time THz imaging system with strong adaptability (*Figure 1D*) (36). The real-time images of samples with micron resolution could be obtained by two-dimensional electro-optical imaging of THz beams (53). Meanwhile, the research has shown that dynamic intensity contour correction is one of the effective ways to achieve real-time THz electro-optical imaging (54).

THz biomedical imaging

Breast tissue

As one of the "invisible killers" of women, breast cancer had about 2.26 million cases worldwide by 2020 (55). Breast conserving surgery (BCS) is a common treatment for early-stage breast cancer with tumors less than 20 cm in size. Pathologists need to perform a histopathological analysis of the excised tissue, which can take about 10 days. However, 15–20% of patients will need to undergo secondary surgery, which not only affects the patient's health but also increases the cost of treatment (56). Therefore, THz imaging, as a non-invasive and rapid imaging technology, can be applied to the detection of breast tumors (57).

The study found that the water content of cancer tissue is higher than that of healthy tissue, and the cancerous area of the sample has a higher RI and absorption coefficient due to the unlimited proliferation of cancer cells (58-60). Therefore, THz imaging can distinguish cancerous tissue from healthy tissue, which provides a fast and effective method for assessing the edge of breast cancer tissue. Bowman *et al.* performed THz imaging of formalin-fixed, paraffin-embedded breast cancer samples (61). The study found that the detection accuracy of the THz system can reach a depth of 1 mm when the tumor is not sliced. This demonstrated the effectiveness of THz in assessing tumor margins. Due to the strong absorption of THz waves in water and the limited penetration depth of THz waves, the reflection mode has been adopted in most studies. The reflection mode is sensitive to small phase changes in the absorption coefficient due to deviations in sliding and tension thickness and non-ideal tension adhesion. By comparing reflection and transmission, it was found that the reflection mode has higher resolution and clearer boundary between different regions (62). Therefore, it is more suitable for imaging of breast tissue. Most THz imaging devices are too bulky, which limits the use of THz imaging devices. Grootendorst *et al.* used a small and simple handheld TPI system to scan 46 cases of freshly excised breast cancer samples *in vitro* with the frequency range of 0.1–1.8 THz. The results showed that the accuracy, sensitivity and specificity of the TPI system for the diagnosis of benign and malignant breast tissue were 87%, 86% and 96% for support vector machine (SVM) and 88%, 87% and 96% for Bayesian, respectively (*Figure 2A*) (63).

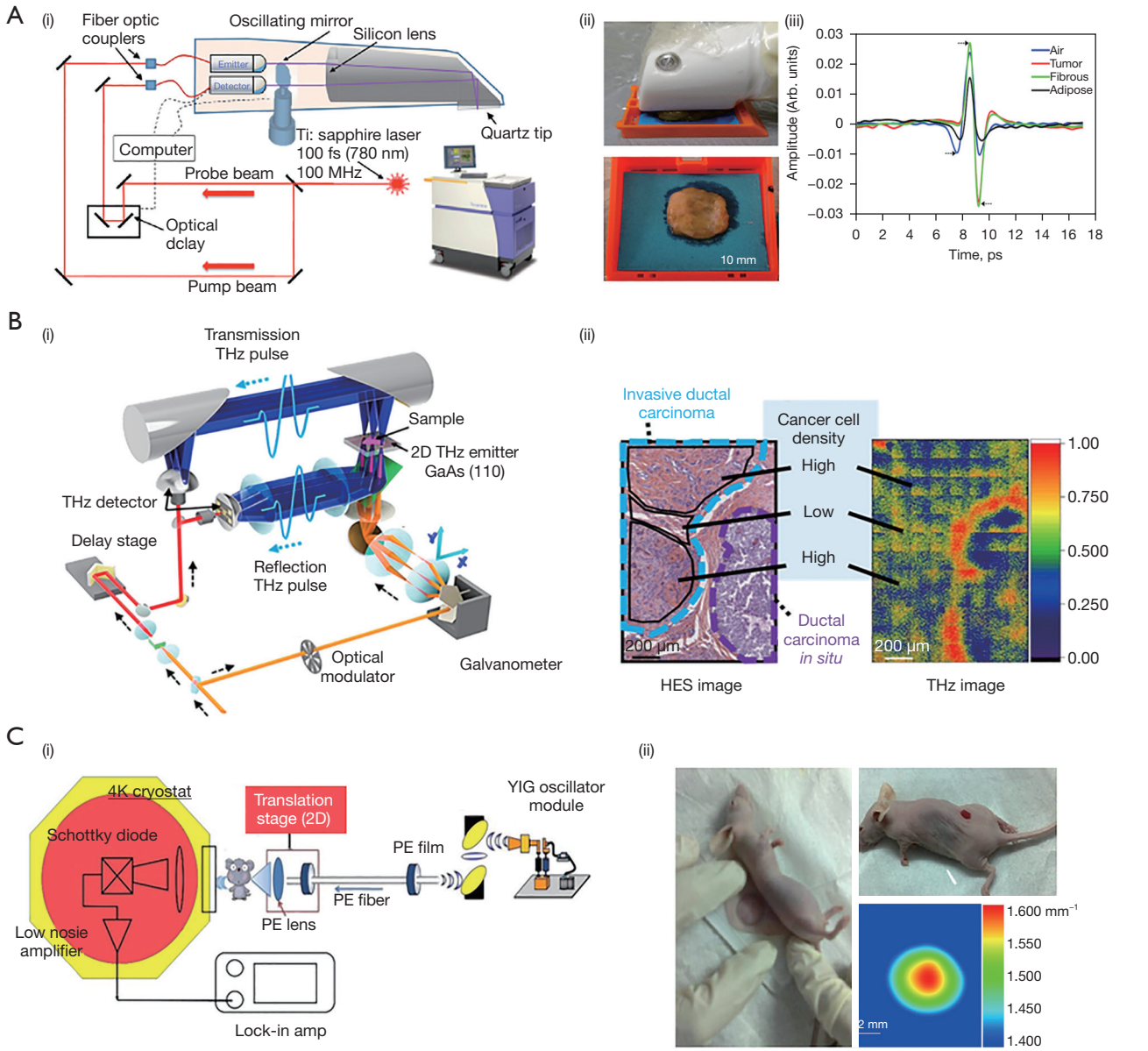

Figure 2 Imaging of breast tissue at THz. (A) (i) Schematic diagram of a THz handheld probe system; (ii) localization of samples for terahertz imaging; (iii) pulse spectra from breast tissue, respectively, for tumors, fibrocytes and adipocytes, and air (63); (B) (i) SPoTS microscope; (ii) comparison of HES and THz images of invasive ductal carcinoma (64); (C) (i) schematic of a system with Schottky diode detectors; (ii) THz images of breast cancer in a mouse model (22). THz, terahertz; HES, hematoxylin-eosin-saffron; PE, polyethylene; YIG, yttrium iron garnet; SPoTS, schematic of scanning point terahertz source.

Using THz technology to image fresh breast tissue in the 300–600 GHz frequency range, Cassar *et al.* demonstrated a clear contrast between breast cancer tissue and healthy tissue (59). This result provided a theoretical basis for THz near-field imaging in the sub-wavelength range. In the same year, Mavarani *et al.* investigated different types and grades of breast cancer tissue using THz reflection imaging at the same frequency (65). The ability to discriminate between different tissues in this frequency range was demonstrated. However, the resolution of THz imaging in the range of 300–600 THz is low. In order to improve the resolution of the image, it was been proposed that the

near-field sensor based on the commercial 0.13 m SiGe-heterojunction bipolar transistor (HBT) technology could be used to improve SNR; in addition, the horizontal resolution could reach 10 m (65,66). This technique can be used to detect tissue with small changes in dielectric constant. In other frequency ranges, compact silicon-based subwavelength THz imagers could be used to accurately image the edge of breast cancer (67). In order to apply THz imaging to biological tissue imaging with inhomogeneous subwavelength scale, Okada *et al.* developed a schematic of scanning point terahertz source (SPoTS) microscope with a spatial resolution of 10 μm (*Figure 2B*) (64). This study proved that the system can observe the inhomogeneity of cells in invasive ductal carcinoma (IDC) through transmission reflection imaging of paraffin-embedded breast cancer tissue, which promotes the application progress of THz technology in biopsy. The maximum detection value of the THz imaging system for tissue is 5 mm, which limits the clinical application. In 2021, Chen *et al.* imaged breast cancer in mouse models at 108 GHz using a THz scanning device constructed by a cryogenic temperature operated Schottky diode detector (*Figure 2C*) (22). The results showed that the detection sensitivity of the detector reached 10–13 W/Hz. The thickness of the detected sample was increased to 8 cm and the volume was less than 1 mm^3.

In recent years, many researches have focused on the automatic localization and classification of breast cancer images. The direction and shape of freshly resected tissue will change when it is examined by histopathology (gold standard technology) after THz imaging. As a result, the THz images and histopathological images cannot be reconciled. Solving the problem of deformation by manual marking caused a waste of human and material resources, so grid modification algorithm was adopted (63,68). However, this method only performs an automatic pixel-by-pixel comparison between the external contours of the THz image and the case image. Bowman *et al.* were the first to apply Bayesian Mixture Model in Markov chain Monte Carlo (MCMC) format to THz image classification, and all THz images had receiver operating characteristic (ROC) area greater than 0.8. It was also the first time that THz imaging was performed on E0771 breast cancer cells (69). Compared with interpolation-based morphing, a mesh morphing algorithm based on homography mapping can capture and correct the complex deformation caused by paraffin embedding, so that the pathological images can be automatically and accurately transformed into the same shape and resolution of the THz image counterpart (70). To evaluate the mesh morphing algorithm, an unsupervised Bayesian learning algorithm based on MCMC was used to classify the samples. The results showed that the area under the ROC of cancer was more than 85% in fresh tissue and more than 77% in formalin-fixed paraffin-embedding (FFPE) tissue. Therefore, this algorithm can provide more effective and accurate evaluation of THz imaging. Bowman *et al.* found that using the Sobel operator for edge detection could well define the tumor boundary, thus enabling automatic processing for THz imaging (61). To realize the automation of tissue classification, the research applied principal component analysis (PCA), artificial neural network (ANN) (accuracy 98.2%; sensitivity 100%; specificity 100%) and K-nearest neighbor (KNN) (accuracy 96.4%; sensitivity 95.1%; specificity 100%) algorithm to THz images, which achieved better tissue classification accuracy and reduced breast cancer detection time (59,71). In addition, the energy to Shannon entropy ratio (ESER) index has been combined with machine learning classifiers for automatic identification of different breast tissues (72). Compared to KNN and SVM, the accuracy, sensitivity and accuracy of ESER were 92.85%, 89.66%, and 96.67% for breast IDC, respectively. Meanwhile, Chavez *et al.* demonstrated that the expectation maximization (EM) algorithm with the low-dimension ordered orthogonal projection (LOOP) method had an accuracy of 74.69% in tissue classification (73). In recent years, researchers have found that a supervised multinomial Bayesian learning method is more suitable for the detection of freshly excised breast cancer samples compared with the existing one-dimensional MCMC and two-dimensional EM (74). Using the above learning methods, the areas under the ROC curves for cancer and muscle reached 92.71% and 86.18% respectively. THz reflection imaging by RI at the frequency of 550 THz has no significance for the classification of low-density malignant edges. To overcome this limitation, Cassar *et al.* combined morphological expansion and RI threshold, which reported the high sensitivity of 80% and specificity of 82% (75).

At present, the main challenges of THz imaging in breast cancer are as follows: (I) the results need to be compared with standard medical imaging tools to verify the effectiveness of THz (76). (II) After THz imaging of freshly excised breast cancer tissue, the direction and shape of the tissue changed during histopathological staining. (III) Excessive fluid around freshly resected tissue causes fluid diffusion of cancer cells, leading to inaccurate classification. (IV) In the resection of breast cancer tumor, doctors can use

THz imaging technology to quickly detect the edge of the tumor, which can avoid a second operation to remove the remaining cancer tissue. However, the dielectric properties of muscle and cancer overlap, and their classification is not accurate (63,69,73), as shown in [*Figure 2A* (iii)]. Therefore, it is very important to improve the differentiation between breast cancer tissue and fibrous tissue. A study has improved the segmentation between tumor tissue and cancer by combining Siamese neural network with multiclass SVM (77). Therefore, machine learning or deep learning can be used to improve the classification accuracy of fibers and cancer. At the same time, metamaterials can also be used to improve the contrast between fibers and cancer tissue. (V) The biological toxicity of THz contrast agent *in vivo* needs to be urgently solved. For *in vivo* THz imaging, contrast agents can be used to improved image contrast. Researchers have investigated THz contrast agents such as metallic nanomaterials, iron oxide nanoparticles, metallic oxide, carbon-based nanomaterials for imaging *in vivo* (10,78-80). However, the biological safety of contrast agents still needs to be constantly explored.

Brain tissue

Brain tissue can be visualized using hematoxylin and eosin (H&E) staining with an optical microscope, which is considered the gold standard. Brain tissue can also be imaged using positron emission tomography (PET) imaging and fluorescence imaging. However, PET imaging requires a positron-emitting radionuclide to be injected into the body, and fluorescence imaging requires a dye to be injected before surgery. The tissue slices are imaged directly using THz technology, which does not require any labelling. Therefore, label-free THz technology can reduce the burden on the body. Recently, studies have shown that label-free THz technology can be used to study brain tissues, such as demyelinating disease (*Figure 3A*) (81,87), Alzheimer's disease (*Figure 3B*) (82,88), brain injury (*Figure 3C*) (83,89,90), glioma, and so on. It provides a new technical method for early diagnosis and formulation of minimally invasive treatment plan (91). Glioma is the most common malignant tumor. Since tumors and normal tissues cannot be accurately identified by white light microscopy, THz technology is one of the techniques that have been used to accurately define the contour of the tumor boundary (92). Due to the higher cell density and water content in brain tumor regions, the RI and absorption coefficient of tumor tissues are higher than those of normal tissues (93,94). Overall, THz technology can be used for differentiation.

THz imaging can reveal different regions of brain tissue compared to other imaging techniques. When this method was used, the tumor area was not only consistent with the pathological section of the H&E-stained image, but also consistent with the tumor area confirmed by green fluorescent protein (GFP) fluorescence image (*Figure 3D*) (84). At the same time, the contour of the tumor margin and the differentiation of different grades of glioma can be clearly shown (95), thus alleviating the bottleneck of incomplete resection rate of low-grade glioma, which is underestimated by protoporphyrin IX (PPIX) fluorescence imaging. The study found that the tumor area in GFP fluorescence imaging was wider than that in THz imaging in the experiment of the living mouse model *in vivo*, which may be due to the diffuse fluorescence signal of tumor deep in the tissue (*Figure 3E*) (84). Up to now, studies have analysed glioma imaging *in vivo* or *in vitro* by using rat and mouse models, and a few studies have used human glioma samples for *in vitro* imaging (10,84,86,96). Wu *et al.* demonstrated that under the high frequency intensity (2.52 THz), THz technology can well discriminate normal tissue from brain glioma tissue *in vivo* or *in vitro* (96).

THz time-domain attenuated total reflection (THz-TD-ATR) spectroscopy mainly consists of the THz-TDS system and the ATR prism (97). In the experiment, the sample is placed on the prism base. The incident THz beam incident undergoes total internal reflection (TIR) at the prism-sample interface, producing an evanescent wave. Compared with transmission and reflection THz imaging, the THz-ATR imaging system can not only reduce the influence of water on the results, but also maintain the characteristics of high sensitivity while ensuring the integrity of sample information. It was found that the continuous THz-ATR imaging system can distinguish tumors in freshly resected brain tissue from normal tissue (98). The effective imaging area of the ATR prism is a key factor for the THz-ATR imaging system. In 2020, Wu *et al.* adopted an isosceles triangle-shaped silicon prism with the base angle of 49 deg and realized that the effective imaging area is equivalent to the imaging area of the prism. Meanwhile, the exit surface of the secondary reflected beam is different from that of single reflection. Therefore, the imaging results will not be affected by the secondary reflected beam (*Figure 3F*) (85). Research has shown that the angle of incidence of THz wave on the prism bottom is 30 deg, and the system has high resolution and stability. Glioma tissues could be well distinguished through the system and were consistent with

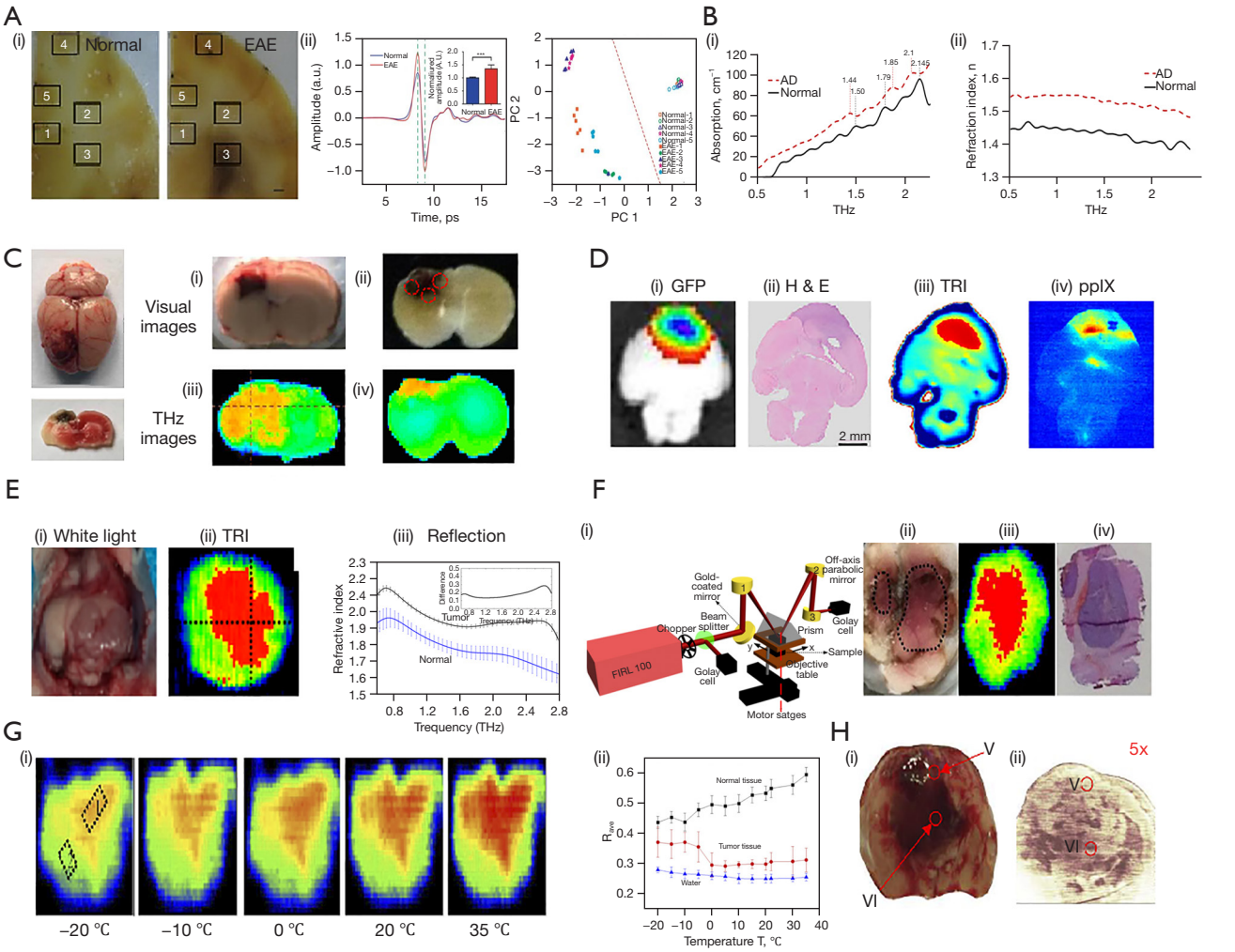

Figure 3 THz imaging of brain tissue. (A) (i) White-field images of paraffin-embedded brain coronal sections from normal and EAE monkeys. "1-5" are the randomly measured five comparable regions of interest. (ii) THz spectra of normal and EAE tissues (81). (B) THz absorption and reflection spectra of AD and normal brain tissue placed on a quartz substrate plate (82). (C) (i,ii) represent visual images of fresh and paraffin-embedded brain tissues, respectively; the three points of the terahertz spectroscopy experiment are shown in red circles. (iii,iv) correspond to its THZ image (83). (D) Images from different imaging modalities (84); (E) imaging of brain tissue from living mice (84); (F) (i) Diagram of experimental equipment; numbers 1–3 in the figure are the off-axis parabolic reflector. THz-ATR was used to distinguish brain tumor tissues from fresh rats: white light (ii), THz-ATR (iii), H&E (iv) the tumor regions marked by dashed lines. (85); (G) (i) effect of temperature on THZ imaging images. Tumor and normal regions, as the marked with dotted boxes 1 and 2. (ii) Reflection spectra of different tissues at different temperatures (86); (H) (i) photo of the freshly-excised tissues; "V" and "VI" are necrosis zone and hemorrhage zone, respectively. (ii) THz microscopy of the freshly-excised tissues (23). ***, P<0.001. R_{ave}: the averaged reflectivity. EAE, experimental autoimmune encephalomyelitis; AD, Alzheimer's disease; THz, terahertz; GFP, green fluorescent protein; H&E, hematoxylin and eosin; TRI, terahertz reflectometry imaging; TPI, THz pulse imaging; ppIX, protoporphyrin IX; ATR, attenuated total reflection.

visual and H&E staining images. By optimizing the ATR prism, the angle of incidence to the bottom of the prism was chosen to be 30 deg. C6-glioma regions of rat brain tissue and U87-glioma regions of mouse brain tissue with different sizes can be well differentiated by THz imaging and are consistent with H&E staining images. This year, Wu *et al.* verified the effect of temperature on the imaging of fresh isolated mouse glioma tissue by using THz

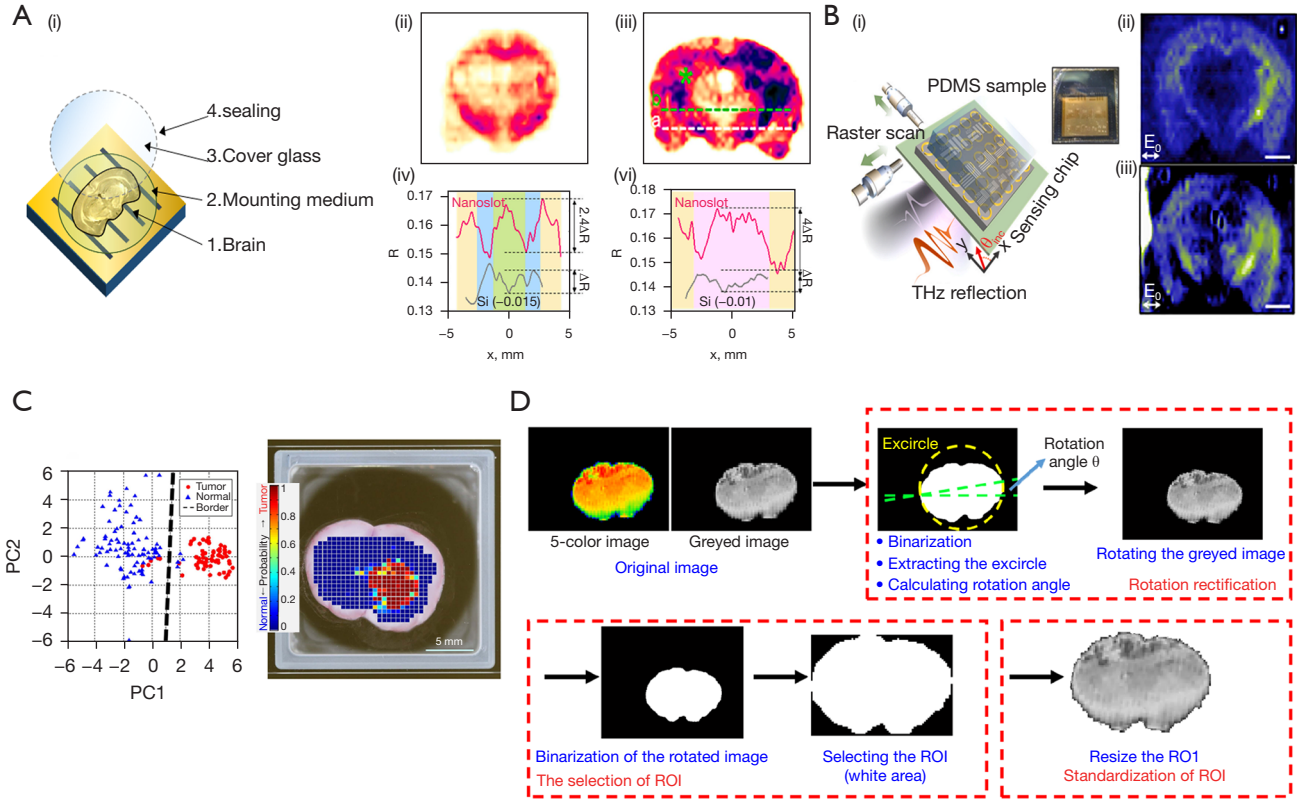

Figure 4 Methods to improve the sensitivity of imaging. (A) (i) Experimental map of metamaterials; THz reflection images using (ii) a bare Si substrate and (iii) a nano-slot chip; reflection values from images (ii) and (iii) along the dashed lines (iv) a and (vi) b (88). The reflectance spectroscopy experiment is performed with the asterisk. (B) (i) Experimental procedure for metamaterial imaging; THz reflection images using (ii) a bare Si substrate and (iii) metamaterials (100). (C) Tumor boundaries obtained by PCA algorithm (93); (D) preprocessing of THz images consisting of rotation rectification (89). PDMS, polydimethylsiloxane; THz, terahertz; ROI, region of interest; PCA, principal component analysis.

ATR imaging system at the frequency of 0.4–2.53 THz (*Figure 3G*) (86). The results showed that the average reflectance of normal tissue increased with increasing temperature, while the reflectance of tumor area showed a decreasing trend. In addition, the average RI and absorption of normal tissue at 20 and −10 ℃ were both smaller than those of tumor tissue. Therefore, it is necessary to select a suitable temperature for THz imaging. The THz near-field imaging system based on the PCAM successfully distinguished the corpus callosum and brain regions of mouse brain tissue (33). This research laid the foundation for the subsequent THz near-field microscope. Solid immersion microscopy is an imaging technique that can overcome the Abbe diffraction limit. This method will improve the resolution of THz imaging, making the image clearer. Imaging of brain tissue with a high-resolution THz solid-state immersion microscope revealed mesoscale spatial fluctuations in THz optical properties due to structural heterogeneity of intact tissue and tumor tissue. The observed THz microscopic images showed heterogeneity of brain tissue in the THz wavelength range (*Figure 3H*) (23). At the same time, the intensity and phase of reflected light through the THz solid immersion microscope were explained using the solid immersion lens reflectivity model. Thus, the RI distribution of fresh rat glioma samples could be reconstructed with sub-wavelength spatial resolution, demonstrating the application potential of the new silicon microscope (99).

In order to better segment tumor tissue and normal tissue, the following two methods can be applied: (I) metamaterials (metasurfaces) were used to enhance the interaction between THz waves and tissue samples, so the contrast of images of normal and tumor tissue is improved (*Figure 4A,4B*) (88,100); (II) machine learning is used to process the THZ image. It mainly includes the following

four steps: image preprocessing; region of interest (ROI) segmentation; feature extraction; pattern classification. In most cases, poor resolution and contrast, as well as noise from devices and the environment, can reduce the quality of THz images and obscure important details needed for accurate segmentation. Therefore, the segmentation of THz images is very important. ROI segmentation of THz images is mainly achieved by image pre-processing through denoising, ROI segmentation, ROI modification and ROI display in the original image. Block matching 3D denoising, fuzzy c-means clustering, morphological operation and Canny edge detection were combined to accurately segment glioma tissues from normal tissues and complex background (101). Using the above method, the accuracy, sensitivity, and specificity of ROI segmentation reached 95.6%, 84.5% and 97.7%, respectively. PCA was used for statistical analysis of THz images to better distinguish normal tissues from tumor tissues (*Figure 4C*) (93). The characteristics of THz images were extracted by combining the spatial transmittance distribution and the normalized gray histogram. Different degrees of traumatic brain injury (TBI) were classified and identified using random forest (RF). The highest classification accuracy was 87.5% (*Figure 4D*) (89). For the detection of mild TBI, RF has a sensitivity of 88.9%. Therefore, it has a lower missed diagnosis rate.

Although normal tissue and tumor tissue can be distinguished by THz imaging technology at present, edematous tissue and tumor tissue cannot be distinguished (95). This leads to unnecessary resection of the patient during surgery. Developments in metamaterials and detector sensitivity are continuously improving image contrast. This makes it easier and more convenient to distinguish between benign and malignant tumors.

Skin tissue

Skin is a flexible outer layer of tissue that covers the body and performs essential functions that have a major impact on health. Many studies on skin tissue have been carried out in the THz range.

In recent years, the advantages of THz radiation in the detection and treatment of dermatauxe and scars have become increasingly prominent. THz imaging of skin tissue is based on the interaction of THz radiation with tissue water, other low-polarity biomolecules, isolated cells and various structural components of the tissue (24). Studies have shown that the RI of hyperplastic scars is significantly higher than that of normal skin using THz imaging (102-104). Fan *et al.* found that THz imaging has great potential for monitoring the wound healing process *in vivo* by observing the 6-month scar recovery process. It could also differentiate between hypertrophic and normal scars (*Figure 5A*) (104). The RI of hypertrophic scars is significantly higher than that of normal skin, whereas the RI of normal scars is the opposite. This study demonstrated the potential of THz as an adjunctive therapy for scars. At the same time, it can also be used to study the healing of skin scars by detecting the water content and its spatial distribution in the skin (108).

At present, three- and four-point classification methods are commonly used for the depth of burns, namely first-degree, superficial second-degree, deep second-degree and third-degree burns. However, this method is mainly diagnosed by doctors according to clinical manifestations, and the accuracy rate is only between 40% and 80%. In addition, the diagnostic techniques used for burn depth mainly include fluorescence detection technology (109), laser Doppler imaging (110,111), polarization-sensitive optical coherence tomography (112), near-infrared spectral imaging technology (113), and so on. In contrast, THz can be used to assess burn wounds *in vitro* and *in vivo* using differences in water content, which is non-ionizing and can be imaged without touching the patient (114). THz imaging has great potential to become a prominent diagnostic technique for burn wound evaluation with high sensitivity and high resolution (115).

Furthermore, skin cancer is usually divided into two main types: non-melanoma skin cancer (NMSC) and malignant melanoma (MM) skin cancer (116). In particular, MM is the most threatening. Although most patients with NMSC can be cured by surgery, the incidence of NMSC is about ten times that of MM (117). The gold standard for removing skin cancer is Mohs micrographic surgery, but it is very time-consuming and costly. THz imaging technology has been shown to have great potential in the diagnosis of skin tissue and related cancers (118). Azizi *et al.* improved the resolution of conventional sensors through photonic band gap (PBG) and a new THz sensor for early detection of skin cancer was developed (119). Melanoma has been reported to be one of the most dangerous skin cancers (24), which has a higher density, higher water content and lower fat content than normal skin. Studies have shown that melanoma has a higher RI and absorption coefficient than normal skin using THz imaging (*Figure 5B*) (105,120,121). Therefore, THz imaging has great potential for early non-invasive diagnosis of MM. The artifacts refer to structures similar to the sample contour caused by frequency-dependent diffraction at the sample edges in THz images. From the THz

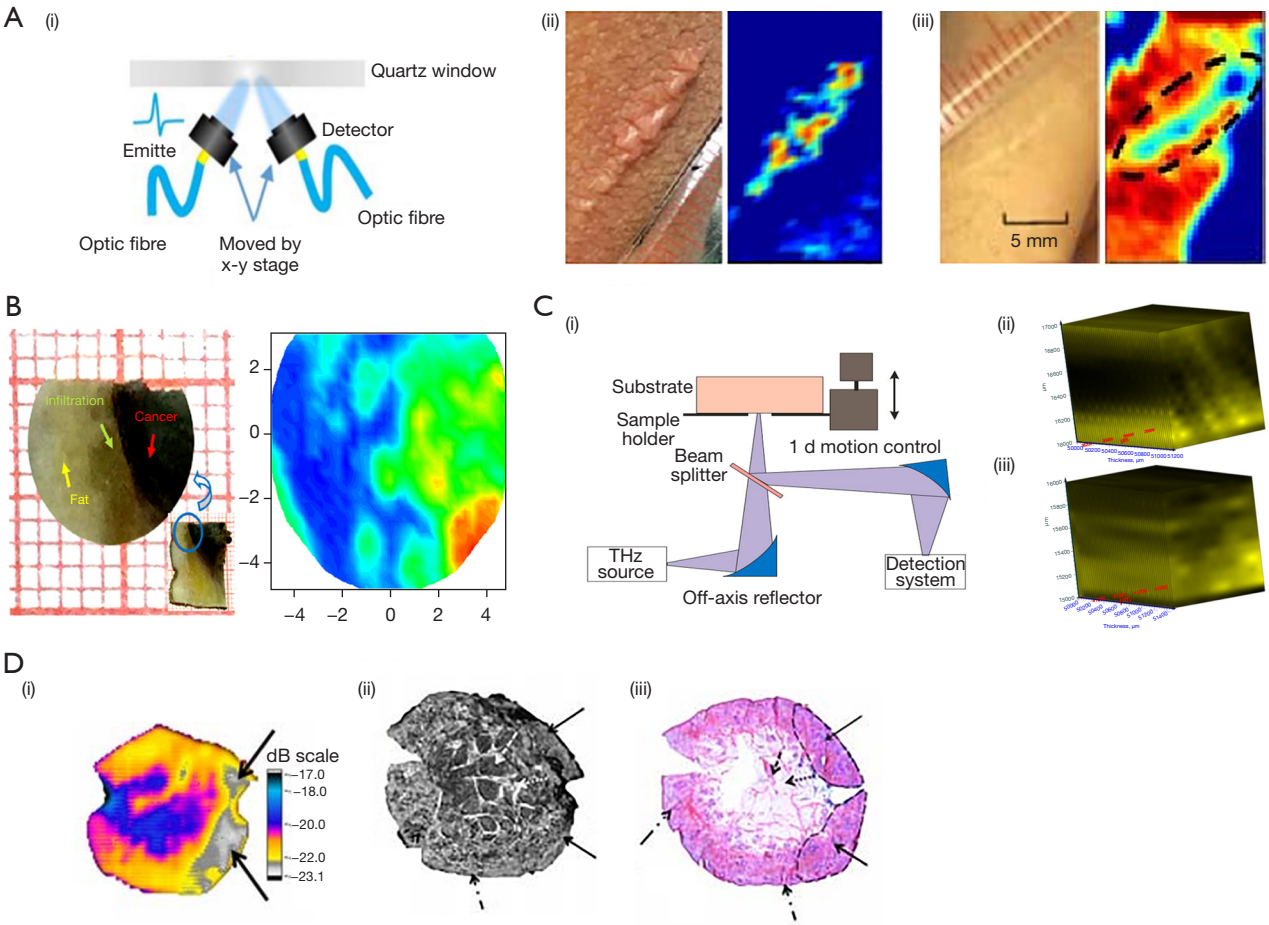

Figure 5 THz imaging of skin tissue. (A) (i) Experiment setup; THz images of hyperplastic (ii) and normal (iii) scars (104). The scar tissue is marked with a black circle. (B) THz imaging of malignant melanoma tissue sections (105). (C) (i) Schematic diagram of the device; slices of the 3D image across the thickness of a healthy skin sample (ii) and basal cell carcinoma skin sample (iii) (106). (D) (i) The cross-polarized THz reflectance image; the location of the tumor is indicated by the arrows; (ii) the cross-polarized optical image; (iii) H&E image (107). Scale bar: 10 mm. THz, terahertz; H&E, hematoxylin and eosin.

intensity image, it was found that the THz power at the edge of the sample was significantly lower than that inside. There is a significant power loss at the edges. Both of the above phenomena can affect the accuracy of the THz image edge. Recently, Yang *et al.* combined Fresnel Kirchhoff diffraction theory with optical aberration to reasonably explain the reason for artifact and large power loss at the THz image edge of melanoma (122). Furthermore, NMSC is the most common cancer in the world, of which basal cell carcinoma is one of the most common skin malignancies. Studies have found that NMSC has higher water content, resulting in lower transmittance than normal skin (123,124). In three-dimensional THz images, normal skin was found to have regular cell patterns, whereas basal cell carcinoma lacked normal cell patterns (*Figure 5C*) (106). This can be used as a basis for early diagnosis. In 2014, Joseph *et al.* combined THz imaging with optical imaging for the first time (*Figure 5D*) (107). The results showed that the image could not only accurately display the morphological features of NMSC, but also accurately identify its edge position.

Water has a strong absorption of THz waves, so the effective penetration of THz is only 0.2–0.3 mm. In the 0.1–2 THz range, 90% of the THz radiation can be retained in the ice for 1 mm, making it possible to image frozen tissue with a thickness of 5 mm. The boundary between frozen and non-frozen tissues shows strong reflection, proving that

THz skin-freezing technology has great potential in skin diagnosis and other applications (125). In addition, THz imaging technology can also show the distribution and penetration of local drugs and detect hydration in the skin (48,126,127). Nevertheless, there are still some defects in the research of skin diseases by THz technology. The most important problem is the lack of penetration depth. Skin cancer can occur in different parts of the human body. In order to achieve real-time imaging of skin cancer, it is also necessary to accelerate the development of rapid movement of imaging systems and complex geometric imaging for different positions in future research (43).

Conclusions

In conclusion, THz imaging technology is developing continuously in biomedicine. Due to the strong absorption effect of water on THz waves, most of the current studies used frozen or paraffin embedded tissue sections and fresh tissue for imaging, which can cause slight damage to the human body. In future research, we should constantly overcome the problem of water absorption and achieve *in vivo* monitoring as soon as possible. At the same time, we need to develop THz systems with better cost effectiveness and detection accuracy. Firstly, THz technology is integrated with emerging technologies such as artificial intelligence and cloud computing, to promote the intelligence and networking of THz technology. THz imaging can use machine learning to realize real-time intelligent identification and detection of objects. Secondly, the repeatability and accuracy of the results can be improved by formulating a standard imaging operation system and establishing a THz database. Finally, metamaterials are applied to improve the interaction between the THZ wave and the target sample as well as the sensitivity of the THZ detector, ultimately achieving better detection accuracy.

THz imaging has been shown to be able to differentiate between benign and malignant tissues, but the treatment recommendations given by clinicians vary widely depending on the stages and type of tumor. Therefore, the sensitivity of the THz imaging system should be continuously improved for the evaluate of the stage and type of tumor (8). Slice thickness, storage conditions, and ice content should be fully considered when establishing the THz database for clinical testing. To improve the sensitivity of THz imaging, THz metamaterials or nanoparticle contrast agents can be used to enhance THz reflection and improve the contrast of images. In addition, materials such as graphene can also be used to improve THz emitters and detectors for better detection performance. At present, the THz endoscope prototype can accurately distinguish tumor tissue, but compact transceivers are still needed for THz technology to be applied in the clinic. In addition, the development of portable and low-cost THz devices is highly beneficial for their application in different clinical situations. At the same time, in order to reduce the effect on detection accuracy caused by the loss of water absorption, microfluidics devices, nanofluidic devices, and THz-ATR systems can be used.

Acknowledgments

Funding: This study was financially supported by the Taishan Scholars Program of Shandong Province (No. TS201712065), Academic Promotion Program of Shandong First Medical University (No. 2019QL009), Science and Technology funding from Jinan (No. 2020GXRC018), Natural Science Foundation of Shandong Province (No. ZR2022QA034), and Talent Introduction Project of Shandong First Medical University (No. YS23-0000041).

Footnote

Reporting Checklist: The authors have completed the Narrative Review reporting checklist. Available at https://qims.amegroups.com/article/view/10.21037/qims-23-526/rc

Conflicts of Interest: All authors have completed the ICMJE uniform disclosure form (available at https://qims.amegroups.com/article/view/10.21037/qims-23-526/coif). The authors have no conflicts of interest to declare.

Ethical Statement: The authors are accountable for all aspects of the work in ensuring that questions related to the accuracy or integrity of any part of the work are appropriately investigated and resolved.

References

1. Rønne C, Keiding SR. Low frequency spectroscopy of liquid water using THz-time domain spectroscopy. J Mol Liq 2002;101:199-218.
2. Berry E, Walker GC, Fitzgerald AJ, Zinov'ev NN, Chamberlain M, Smye SW, Miles RE, Smith MA. Do in vivo terahertz imaging systems comply with safety guidelines? J Laser Appl 2003;15:192-8.
3. Burford NM, El-Shenawee MO. Review of terahertz photoconductive antenna technology. Optical Engineering 2017;56:010901.
4. Afsah-Hejri L, Hajeb P, Ara P, Ehsani RJ. A Comprehensive Review on Food Applications of Terahertz Spectroscopy and Imaging. Compr Rev Food Sci Food Saf 2019;18:1563-621.
5. Feng CH, Otani C. Terahertz spectroscopy technology as an innovative technique for food: Current state-of-the-Art research advances. Crit Rev Food Sci Nutr 2021;61:2523-43.
6. Afsah-Hejri L, Akbari E, Toudeshki A, Homayouni T, Alizadeh A, Ehsani R. Terahertz spectroscopy and imaging: A review on agricultural applications. Comput Electron Agric 2020;177:105628.
7. Ge H, Lv M, Lu X, Jiang Y, Wu G, Li G, Li L, Li Z, Zhang Y. Applications of THz Spectral Imaging in the Detection of Agricultural Products. Photonics 2021;8:518.
8. Yang X, Zhao X, Yang K, Liu Y, Liu Y, Fu W, Luo Y. Biomedical Applications of Terahertz Spectroscopy and Imaging. Trends Biotechnol 2016;34:810-24.
9. Wan M, Healy JJ, Sheridan JT. Terahertz phase imaging and biomedical applications. Optics & Laser Technology 2020;122:105859.
10. Yan Z, Zhu LG, Meng K, Huang W, Shi Q. THz medical imaging: from in vitro to in vivo. Trends Biotechnol 2022;40:816-30.
11. Li T, Zhang L, HE JA, Zhang SX, Gu DY. Terahertz Time-Domain Spectroscopy for Identification of Hazardous Substances in Mail. Spectroscopy and spectral analysis 2019;39:3724-30.
12. Hirata A, Yaita M. Ultrafast Terahertz Wireless Communications Technologies. IEEE Trans Terahertz Sci Technol 2015;5:1128-32.
13. Feng W, Wei ST, Cao JC. 6G technology development vision and terahertz communication. Acta Physica Sinica 2021;70:244303.
14. Yu L, Hao L, Meiqiong T, Jiaoqi H, Wei L, Jinying D, Xueping C, Weiling F, Yang Z. The medical application of terahertz technology in non-invasive detection of cells and tissues: opportunities and challenges. RSC Adv 2019;9:9354-63.
15. Mcclatchey K, Reiten MT, Cheville RA. Time resolved synthetic aperture terahertz impulse imaging. Appl Phys Lett 2001;79:4485-7.
16. Wang M, Zhang Y, Guo L, Lv M, Wang P, Wang X. Spintronics Based Terahertz Sources. Crystals 2022;12:1661.
17. Fülöp JA, Tzortzakis S, Kampfrath T. Laser-Driven Strong-Field Terahertz Sources. Adv Optical Mater 2020;8:1900681.
18. Vitiello MS, De Natale P. Terahertz Quantum Cascade Lasers as Enabling Quantum Technology. Adv Quantum Technol 2022;5:2100082.
19. Tantiwanichapan K, Durmaz H. Improvement of Response Time and Heat-Transfer Capacity of Metamaterial Absorber for Terahertz Detector Applications. IEEE Sensors Journal 2023;23:4700-6.
20. Jacoby M. Biomedical terahertz imaging advances in far-infrared spectroscopy could aid cancer diagnosis. Chem Eng News 2015;93:10-4.
21. Chen H, Chen TH, Tseng TF, Lu JT, Kuo CC, Fu SC, Lee WJ, Tsai YF, Huang YY, Chuang EY, Hwang YJ, Sun CK. High-sensitivity in vivo THz transmission imaging of early human breast cancer in a subcutaneous xenograft mouse model. Opt Express 2011;19:21552-62.
22. Chen H, Han J, Wang D, Zhang Y, Li X, Chen X. In vivo Estimation of Breast Cancer Tissue Volume in Subcutaneous Xenotransplantation Mouse Models by Using a High-Sensitivity Fiber-Based Terahertz Scanning Imaging System. Front Genet 2021;12:700086.
23. Kucheryavenko AS, Chernomyrdin NV, Gavdush AA, Alekseeva AI, Nikitin PV, Dolganova IN, Karalkin PA, Khalansky AS, Spektor IE, Skorobogatiy M, Tuchin VV, Zaytsev KI. Terahertz dielectric spectroscopy and solid immersion microscopy of ex vivo glioma model 101.8: brain tissue heterogeneity. Biomed Opt Express 2021;12:5272-89.
24. Nikitkina AI, Bikmulina PY, Gafarova ER, Kosheleva NV, Efremov YM, Bezrukov EA, Butnaru DV, Dolganova IN, Chernomyrdin NV, Cherkasova OP, Gavdush AA, Timashev PS. Terahertz radiation and the skin: a review. J Biomed Opt 2021;26:043005.
25. Rong L, Latychevskaia T, Chen C, Wang D, Yu Z, Zhou X, Li Z, Huang H, Wang Y, Zhou Z. Terahertz in-line digital holography of human hepatocellular carcinoma tissue. Sci Rep 2015;5:8445.

26. Vafapour Z, Keshavarz A, Ghahraloud H. The potential of terahertz sensing for cancer diagnosis. Heliyon 2020;6:e05623.
27. Hernandez-Cardoso GG, Rojas-Landeros SC, Alfaro-Gomez M, Hernandez-Serrano AI, Salas-Gutierrez I, Lemus-Bedolla E, Castillo-Guzman AR, Lopez-Lemus HL, Castro-Camus E. Terahertz imaging for early screening of diabetic foot syndrome: A proof of concept. Sci Rep 2017;7:42124.
28. Freer S, Sui C, Hanham SM, Grover LM, Navarro-Cía M. Hybrid reflection retrieval method for terahertz dielectric imaging of human bone. Biomed Opt Express 2021;12:4807-20.
29. Shi W, Wang Y, Hou L, Ma C, Yang L, Dong C, Wang Z, Wang H, Guo J, Xu S, Li J. Detection of living cervical cancer cells by transient terahertz spectroscopy. J Biophotonics 2021;14:e202000237.
30. Federici JF, Mitrofanov O, Lee M, Hsu JW, Brener I, Harel R, Wynn JD, Pfeiffer LN, West KW. Terahertz near-field imaging. Phys Med Biol 2002;47:3727-34.
31. van der Valk NCJ, Planken PCM. Electro-optic detection of subwavelength terahertz spot sizes in the near field of a metal tip. Appl Phys Lett 2002;81:1558-60.
32. Okada K, Serita K, Zang Z, Murakami H, Kawayama I, Cassar Q, Macgrogan G, Guillet JP, Mounaix P, Tonouchi M. Scanning laser terahertz near-field reflection imaging system. Appl Phys Express 2019;12:122005.
33. Geng G, Dai G, Li D, Zhou S, Li Z, Yang Z, Xu Y, Han J, Chang T, Cui HL, Wang H. Imaging brain tissue slices with terahertz near-field microscopy. Biotechnol Prog 2019;35:e2741.
34. Li Z, Yan S, Zang Z, Geng G, Yang Z, Li J, Wang L, Yao C, Cui HL, Chang C, Wang H. Single cell imaging with near-field terahertz scanning microscopy. Cell Prolif 2020;53:e12788.
35. She R, Liu W, Lu Y, Zhou Z, Li G. Fourier single-pixel imaging in the terahertz regime. Appl Phys Lett 2019;115:021101.
36. Zolliker P, Shalaby M, Söllinger E, Mavrona E, Hack E. Real-Time High Resolution THz Imaging with a Fiber-Coupled Photo Conductive Antenna and an Uncooled Microbolometer Camera. Sensors (Basel) 2021;21:3757.
37. Chen X, Hu D, Mescall R, You G, Basov DN, Dai Q, Liu M. Modern Scattering-Type Scanning Near-Field Optical Microscopy for Advanced Material Research. Adv Mater 2019;31:e1804774.
38. Yang Z, Tang D, Hu J, Tang M, Zhang M, Cui HL, Wang L, Chang C, Fan C, Li J, Wang H. Near-Field Nanoscopic Terahertz Imaging of Single Proteins. Small 2021;17:e2005814.
39. Vallés A, He J, Ohno S, Omatsu T, Miyamoto K. Broadband high-resolution terahertz single-pixel imaging. Opt Express 2020;28:28868-81.
40. Sun MJ, Zhang JM. Single-Pixel Imaging and Its Application in Three-Dimensional Reconstruction: A Brief Review. Sensors (Basel) 2019;19:732.
41. Zanotto L, Piccoli R, Dong J, Caraffini D, Morandotti R, Razzari L. Time-domain terahertz compressive imaging. Opt Express 2020;28:3795-802.
42. Chan WL, Charan K, Takhar D, Kelly KF, Baraniuk RG, Mittleman DM. A single-pixel terahertz imaging system based on compressed sensing. Appl Phys Lett 2008;93:121105.
43. Shang Y, Wang X, Sun W, Han P, Ye J, Feng S, Zhang Y. Terahertz image reconstruction based on compressed sensing and inverse Fresnel diffraction. Opt Express 2019;27:14725-35.
44. Stantchev RI, Yu X, Blu T, Pickwell-MacPherson E. Real-time terahertz imaging with a single-pixel detector. Nat Commun 2020;11:2535.
45. Mohr T, Herdt A, Elsässer W. 2D tomographic terahertz imaging using a single pixel detector. Opt Express 2018;26:3353-67.
46. Li W, Hu X, Wu J, Fan K, Chen B, Zhang C, Hu W, Cao X, Jin B, Lu Y, Chen J, Wu P. Dual-color terahertz spatial light modulator for single-pixel imaging. Light Sci Appl 2022;11:191.
47. Kowalski M. Real-time concealed object detection and recognition in passive imaging at 250 GHz. Appl Opt 2019;58:3134-40.
48. Lindley-Hatcher H, Stantchev RI, Chen X, Hernandez-Serrano AI, Hardwicke J, Pickwell-MacPherson E. Real time THz imaging—opportunities and challenges for skin cancer detection. Appl Phys Lett 2021;118:230501.
49. Guerboukha H, Nallappan K, Skorobogatiy M. Toward real-time terahertz imaging. Adv Opt Photonics 2018;10:843-938.
50. Kanda N, Konishi K, Nemoto N, Midorikawa K, Kuwata-Gonokami M. Real-time broadband terahertz spectroscopic imaging by using a high-sensitivity terahertz camera. Sci Rep 2017;7:42540.
51. Wen Y, Jia D, Ma W, Feng Y, Liu M, Dong L, Zhao Y, Yu X. Photomechanical meta-molecule array for real-time terahertz imaging. Microsyst Nanoeng 2017;3:17071.
52. Perraud JB, Guillet JP, Redon O, Hamdi M, Simoens F, Mounaix P. Shape-from-focus for real-time terahertz 3D

imaging. Opt Lett 2019;44:483-6.
53. Blanchard F, Tanaka K. Improving time and space resolution in electro-optic sampling for near-field terahertz imaging. Opt Lett 2016;41:4645-8.
54. Blanchard F, Arikawa T, Tanaka K. Real-Time Megapixel Electro-Optical Imaging of THz Beams with Probe Power Normalization. Sensors (Basel) 2022;22:4482.
55. Wilkinson L, Gathani T. Understanding breast cancer as a global health concern. Br J Radiol 2022;95:20211033.
56. Ashworth PC, O'Kelly P, Purushotham AD, Pinder SE, Kontos M, Pepper M, Wallace VP. An intra-operative THz probe for use during the surgical removal of breast tumors. 2008 33rd International Conference on Infrared, Millimeter and Terahertz Waves. Pasadena, CA, USA: IEEE; 2008:1-3.
57. Wang L. Terahertz Imaging for Breast Cancer Detection. Sensors (Basel) 2021;21:6465.
58. Ashworth PC, Pickwell-MacPherson E, Provenzano E, Pinder SE, Purushotham AD, Pepper M, Wallace VP. Terahertz pulsed spectroscopy of freshly excised human breast cancer. Opt Express 2009;17:12444-54.
59. Cassar Q, Al-Ibadi A, Mavarani L, Hillger P, Grzyb J, MacGrogan G, Zimmer T, Pfeiffer UR, Guillet JP, Mounaix P. Pilot study of freshly excised breast tissue response in the 300-600 GHz range. Biomed Opt Express 2018;9:2930-42.
60. Vohra N, Bowman T, Bailey K, El-Shenawee M. Terahertz Imaging and Characterization Protocol for Freshly Excised Breast Cancer Tumors. J Vis Exp 2020;(158):10.3791/61007.
61. Bowman T, Wu Y, Gauch J, Campbell LK, El-Shenawee M. Terahertz Imaging of Three-Dimensional Dehydrated Breast Cancer Tumors. J Infrared Millim Terahertz Waves 2017;38:766-86.
62. Bowman T, El-Shenawee M, Campbell LK. Terahertz transmission vs reflection imaging and model-based characterization for excised breast carcinomas. Biomed Opt Express 2016;7:3756-83.
63. Grootendorst MR, Fitzgerald AJ, Brouwer de Koning SG, Santaolalla A, Portieri A, Van Hemelrijck M, Young MR, Owen J, Cariati M, Pepper M, Wallace VP, Pinder SE, Purushotham A. Use of a handheld terahertz pulsed imaging device to differentiate benign and malignant breast tissue. Biomed Opt Express 2017;8:2932-45.
64. Okada K, Cassar Q, Murakami H, MacGrogan G, Guillet JP, Mounaix P, Tonouchi M, Serita K. Label-Free Observation of Micrometric Inhomogeneity of Human Breast Cancer Cell Density Using Terahertz Near-Field Microscopy. Photonics 2021;8:151.
65. Mavarani L, Hillger P, Bücher T, Grzyb J, Pfeiffer U, Cassar Q, Al-Ibadi A, Zimmer T, Guillet J, Mounaix P, MacGrogan G. NearSense – Advances Towards a Silicon-Based Terahertz Near-Field Imaging Sensor for Ex Vivo Breast Tumour Identification. Frequenz 2018;72:93-9.
66. Grzyb J, Heinemann B, Pfeiffer UR. A 0.55 THz Near-Field Sensor With a μm -Range Lateral Resolution Fully Integrated in 130 nm SiGe BiCMOS. IEEE J Solid-State Circuits 2016;51:3063-77.
67. Pfeiffer UR, Hillger P, Jain R, Grzyb J, Bucher T, Cassar Q, MacGrogan G, Guillet JP, Mounaix P, Zimmer T. Ex Vivo Breast Tumor Identification: Advances Toward a Silicon-Based Terahertz Near-Field Imaging Sensor. IEEE Microwave Magazine 2019;20:32-46.
68. Henry SC, Zurk LM, Schecklman S. Terahertz spectral imaging using correlation processing. IEEE Trans Terahertz Sci Technol 2013;3:486-93.
69. Bowman T, Chavez T, Khan K, Wu J, Chakraborty A, Rajaram N, Bailey K, El-Shenawee M. Pulsed terahertz imaging of breast cancer in freshly excised murine tumors. J Biomed Opt 2018;23:1-13.
70. Chavez T, Bowman T, Wu J, Bailey K, El-Shenawee M. Assessment of Terahertz Imaging for Excised Breast Cancer Tumors with Image Morphing. J Infrared Millim Terahertz Waves 2018;39:1283-302.
71. Hassan JM, Hakeem SI. Detection and Classification of Breast Cancer Based-On Terahertz Imaging Technique Using Artificial Neural Network & K-Nearest Neighbor Algorithm. Int J Appl Eng Res 2017;12:10661-8.
72. Liu W, Zhang R, Ling Y, Tang H, She R, Wei G, Gong X, Lu Y. Automatic recognition of breast invasive ductal carcinoma based on terahertz spectroscopy with wavelet packet transform and machine learning. Biomed Opt Express 2020;11:971-81.
73. Chavez T, Vohra N, Wu J, Bailey K, El-Shenawee M. Breast Cancer Detection with Low-dimension Ordered Orthogonal Projection in Terahertz Imaging. IEEE Trans Terahertz Sci Technol 2020;10:176-89.
74. Chavez T, Vohra N, Bailey K, El-Shenawee M, Wu J. Supervised Bayesian learning for breast cancer detection in terahertz imaging. Biomed Signal Process Control 2021;70:102949.
75. Cassar Q, Caravera S, MacGrogan G, Bücher T, Hillger P, Pfeiffer U, Zimmer T, Guillet JP, Mounaix P. Terahertz refractive index-based morphological dilation for breast carcinoma delineation. Sci Rep 2021;11:6457.
76. Bowman T, El-Shenawee M, Bailey K. Challenges in

Terahertz Imaging of Freshly Excised Human Breast Tumors. 2018 IEEE International Symposium on Antennas and Propagation & USNC/URSI National Radio Science Meeting. Boston, MA, USA: IEEE; 2018:13-4.
77. Liu H, Vohra N, Bailey K, El-Shenawee M, Nelson AH. Deep Learning Classification of Breast Cancer Tissue from Terahertz Imaging Through Wavelet Synchro-Squeezed Transformation and Transfer Learning. J Infrared Millim Terahertz Waves 2022;43:48-70.
78. Oh SJ, Choi J, Maeng I, Park JY, Lee K, Huh YM, Suh JS, Haam S, Son JH. Molecular imaging with terahertz waves. Opt Express 2011;19:4009-16.
79. Zhang R, Zhang L, Wu T, Zuo S, Wang R, Zhang C, Zhang J, Fang J. Contrast-enhanced continuous-terahertz-wave imaging based on superparamagnetic iron oxide nanoparticles for biomedical applications. Opt Express 2016;24:7915-21.
80. Bowman T, Walter A, Shenderova O, Nunn N, McGuire G, El-Shenawee M. A Phantom Study of Terahertz Spectroscopy and Imaging of Micro- and Nano-diamonds and Nano-onions as Contrast Agents for Breast Cancer. Biomed Phys Eng Express 2017;3:055001.
81. Zou Y, Li J, Cui Y, Tang P, Du L, Chen T, Meng K, Liu Q, Feng H, Zhao J, Chen M, Zhu LG. Terahertz Spectroscopic Diagnosis of Myelin Deficit Brain in Mice and Rhesus Monkey with Chemometric Techniques. Sci Rep 2017;7:5176.
82. Shi L, Shumyatsky P, Rodríguez-Contreras A, Alfano R. Terahertz spectroscopy of brain tissue from a mouse model of Alzheimer's disease. J Biomed Opt 2016;21:15014.
83. Zhao H, Wang Y, Chen L, Shi J, Ma K, Tang L, Xu D, Yao J, Feng H, Chen T. High-sensitivity terahertz imaging of traumatic brain injury in a rat model. J Biomed Opt 2018;23:1-7.
84. Ji YB, Oh SJ, Kang SG, Heo J, Kim SH, Choi Y, Song S, Son HY, Kim SH, Lee JH, Haam SJ, Huh YM, Chang JH, Joo C, Suh JS. Terahertz reflectometry imaging for low and high grade gliomas. Sci Rep 2016;6:36040.
85. Wu L, Xu D, Wang Y, Zhang Y, Wang H, Liao B, Gong S, Chen T, Wu N, Feng H, Yao J. Horizontal-scanning attenuated total reflection terahertz imaging for biological tissues. Neurophotonics 2020;7:025005.
86. Wu L, Wang Y, Liao B, Zhao L, Chen K, Ge M, Li H, Chen T, Feng H, Xu D, Yao J. Temperature dependent terahertz spectroscopy and imaging of orthotopic brain gliomas in mouse models. Biomed Opt Express 2022;13:93-104.
87. Oh SJ, Kim SH, Ji YB, Jeong K, Park Y, Yang J, Park DW, Noh SK, Kang SG, Huh YM, Son JH, Suh JS. Study of freshly excised brain tissues using terahertz imaging. Biomed Opt Express 2014;5:2837-42.
88. Lee SH, Shin S, Roh Y, Oh SJ, Lee SH, Song HS, Ryu YS, Kim YK, Seo M. Label-free brain tissue imaging using large-area terahertz metamaterials. Biosens Bioelectron 2020;170:112663.
89. Shi J, Wang Y, Chen T, Xu D, Zhao H, Chen L, Yan C, Tang L, He Y, Feng H, Yao J. Automatic evaluation of traumatic brain injury based on terahertz imaging with machine learning. Opt Express 2018;26:6371-81.
90. Wang Y, Wang G, Xu D, Jiang B, Ge M, Wu L, Yang C, Mu N, Wang S, Chang C, Chen T, Feng H, Yao J. Terahertz spectroscopic diagnosis of early blast-induced traumatic brain injury in rats. Biomed Opt Express 2020;11:4085-98.
91. Cherkasova O, Peng Y, Konnikova M, Kistenev Y, Shi C, Vrazhnov D, Shevelev O, Zavjalov E, Kuznetsov S, Shkurinov A. Diagnosis of Glioma Molecular Markers by Terahertz Technologies. Photonics 2021;8:22.
92. Ostrom QT, Bauchet L, Davis FG, Deltour I, Fisher JL, Langer CE, Pekmezci M, Schwartzbaum JA, Turner MC, Walsh KM, Wrensch MR, Barnholtz-Sloan JS. The epidemiology of glioma in adults: a "state of the science" review. Neuro Oncol 2014;16:896-913.
93. Yamaguchi S, Fukushi Y, Kubota O, Itsuji T, Ouchi T, Yamamoto S. Brain tumor imaging of rat fresh tissue using terahertz spectroscopy. Sci Rep 2016;6:30124.
94. Gavdush AA, Chernomyrdin NV, Komandin GA, Dolganova IN, Nikitin PV, Musina GR, Katyba GM, Kucheryavenko AS, Reshetov IV, Potapov AA, Tuchin VV, Zaytsev KI. Terahertz dielectric spectroscopy of human brain gliomas and intact tissues ex vivo: double-Debye and double-overdamped-oscillator models of dielectric response. Biomed Opt Express 2021;12:69-83.
95. Gavdush AA, Chernomyrdin NV, Malakhov KM, Beshplav ST, Dolganova IN, Kosyrkova AV, Nikitin PV, Musina GR, Katyba GM, Reshetov IV, Cherkasova OP, Komandin GA, Karasik VE, Potapov AA, Tuchin VV, Zaytsev KI. Terahertz spectroscopy of gelatin-embedded human brain gliomas of different grades: a road toward intraoperative THz diagnosis. J Biomed Opt 2019;24:1-5.
96. Wu L, Xu D, Wang Y, Liao B, Jiang Z, Zhao L, Sun Z, Wu N, Chen T, Feng H, Yao J. Study of in vivo brain glioma in a mouse model using continuous-wave terahertz reflection imaging. Biomed Opt Express 2019;10:3953-62.
97. Huang Y, Singh R, Xie L, Ying Y. Attenuated Total Reflection for Terahertz Modulation, Sensing,

Spectroscopy and Imaging Applications: A Review. Appl Sci 2020;10:4688.
98. Li J, Liu M, Gao J, Jiang Y, Wu L, Cheong YK, Ren G, Yang Z. AVNP2 protects against cognitive impairments induced by C6 glioma by suppressing tumour associated inflammation in rats. Brain Behav Immun 2020;87:645-59.
99. Chernomyrdin NV, Skorobogatiy MA, Gavdush AA, Musina GR, Katyba GM, Komandin GA, Khorokhorov AM, Spektor IE, Tuchin VV, Zaytsev KI. Quantitative super-resolution solid immersion microscopy via refractive index profile reconstruction. Optica 2021;8:1471-80.
100. Roh Y, Lee SH, Kwak J, Song HS, Shin S, Kim YK, Wu JW, Ju BK, Kang B, Seo M. Terahertz imaging with metamaterials for biological applications. Sens Actuators B Chem 2022;352:130993.
101. Wang Y, Sun Z, Xu D, Wu L, Chang J, Tang L, Jiang Z, Jiang B, Wang G, Chen T, Feng H, Yao J. A hybrid method based region of interest segmentation for continuous wave terahertz imaging. J Phys D Appl Phys 2020;53:095403.
102. Bajwa N, Au J, Jarrahy R, Sung S, Fishbein MC, Riopelle D, Ennis DB, Aghaloo T, St John MA, Grundfest WS, Taylor ZD. Non-invasive terahertz imaging of tissue water content for flap viability assessment. Biomed Opt Express 2017;8:460-74.
103. Woodward RM, Cole BE, Wallace VP, Pye RJ, Arnone DD, Linfield EH, Pepper M. Terahertz pulse imaging in reflection geometry of human skin cancer and skin tissue. Phys Med Biol 2002;47:3853-63.
104. Fan S, Ung BSY, Parrott EPJ, Wallace VP, Pickwell-MacPherson E. In vivo terahertz reflection imaging of human scars during and after the healing process. J Biophotonics 2017;10:1143-51.
105. Li J, Xie Y, Sun P. Edge detection on terahertz pulse imaging of dehydrated cutaneous malignant melanoma embedded in paraffin. Front Optoelectron 2019;12:317-23.
106. Rahman A, Rahman AK, Rao B. Early detection of skin cancer via terahertz spectral profiling and 3D imaging. Biosens Bioelectron 2016;82:64-70.
107. Joseph CS, Patel R, Neel VA, Giles RH, Yaroslavsky AN. Imaging of ex vivo nonmelanoma skin cancers in the optical and terahertz spectral regions optical and terahertz skin cancers imaging. J Biophotonics 2014;7:295-303.
108. Sun Q, Parrott EPJ, Pickwell-Macpherson E. In vivo estimation of the water diffusivity in occluded human skin using terahertz rejection spectroscopy. 2017 42nd International Conference on Infrared, Millimeter, and Terahertz Waves (IRMMW-THz). Cancun: IEEE; 2017.
109. Fourman MS, Phillips BT, Crawford L, McClain SA, Lin F, Thode HC Jr, Dagum AB, Singer AJ, Clark RA. Indocyanine green dye angiography accurately predicts survival in the zone of ischemia in a burn comb model. Burns 2014;40:940-6.
110. Hoeksema H, Baker RD, Holland AJ, Perry T, Jeffery SL, Verbelen J, Monstrey S. A new, fast LDI for assessment of burns: a multi-centre clinical evaluation. Burns 2014;40:1274-82.
111. Venclauskiene A, Basevicius A, Zacharevskij E, Vaicekauskas V, Rimdeika R, Lukosevicius S. Laser Doppler imaging as a tool in the burn wound treatment protocol. Wideochir Inne Tech Maloinwazyjne 2014;9:24-30.
112. Kim KH, Pierce MC, Maguluri G, Park BH, Yoon SJ, Lydon M, Sheridan R, de Boer JF. In vivo imaging of human burn injuries with polarization-sensitive optical coherence tomography. J Biomed Opt 2012;17:066012.
113. Seki T, Fujioka M, Fukushima H, Matsumori H, Maegawa N, Norimoto K, Okuchi K. Regional tissue oxygen saturation measured by near-infrared spectroscopy to assess the depth of burn injuries. Int J Burns Trauma 2014;4:40-4.
114. Li S, Mohamedi AH, Senkowsky J, Nair A, Tang L. Imaging in Chronic Wound Diagnostics. Adv Wound Care (New Rochelle) 2020;9:245-63.
115. Dutta M, Bhalla AS, Guo R. THz Imaging of Skin Burn: Seeing the Unseen-An Overview. Adv Wound Care (New Rochelle) 2016;5:338-48.
116. Mueller CS, Reichrath J. Histology of melanoma and nonmelanoma skin cancer. Adv Exp Med Biol 2008;624:215-26.
117. Zhu S, Sun C, Zhang L, Du X, Tan X, Peng S. Incidence Trends and Survival Prediction of Malignant Skin Cancer: A SEER-Based Study. Int J Gen Med 2022;15:2945-56.
118. Keshavarz A, Vafapour Z. Water-Based Terahertz Metamaterial for Skin Cancer Detection Application. IEEE Sensors Journal 2018;19:1519-24.
119. Azizi S, Nouri-Novin S, Seyedsharbaty MM, Zarrabi FB. Early skin cancer detection sensor based on photonic band gap and graphene load at terahertz regime. Opt Quant Electron 2018;50:230.
120. Li D, Yang Z, Fu A, Chen T, Chen L, Tang M, Zhang H, Mu N, Wang S, Liang G, Wang H. Detecting melanoma with a terahertz spectroscopy imaging technique. Spectrochim Acta A Mol Biomol Spectrosc 2020;234:118229.
121. Zhang R, Yang K, Abbasi Q, Abuali NA, Alomainy A. Experimental Characterization of Artificial Human Skin

with Melanomas for Accurate Modelling and Detection in Healthcare Application. 2018 43rd International Conference on Infrared, Millimeter, and Terahertz Waves (IRMMW-THz2018). Nagoya: IEEE; 2018.
122. Yang Z, Zhang M, Li D, Chen L, Fu A, Liang Y, Wang H. Study on an artificial phenomenon observed in terahertz biological imaging. Biomed Opt Express 2021;12:3133-41.
123. Joseph CS, Yaroslavsky AN, Neel VA, Goyette TM, Giles RH. Continuous wave terahertz transmission imaging of nonmelanoma skin cancers. Lasers Surg Med 2011;43:457-62.
124. Niculet E, Craescu M, Rebegea L, Bobeica C, Nastase F, Lupasteanu G, Stan DJ, Chioncel V, Anghel L, Lungu M, Tatu AL. Basal cell carcinoma: Comprehensive clinical and histopathological aspects, novel imaging tools and therapeutic approaches (Review). Exp Ther Med 2022;23:60.
125. Vilagosh Z, Lajevardipour A, Wood AW. Computational phantom study of frozen melanoma imaging at 0.45 terahertz. Bioelectromagnetics 2019;40:118-27.
126. Kim KW, Kim KS, Kim H, Lee SH, Park JH, Han JH, Seok SH, Park J, Choi Y, Kim YI, Han JK, Son JH. Terahertz dynamic imaging of skin drug absorption. Opt Express 2012;20:9476-84.
127. Wang L, Guilavogui S, Yin H, Wu Y, Zang X, Xie J, Ding L, Chen L. Critical Factors for In Vivo Measurements of Human Skin by Terahertz Attenuated Total Reflection Spectroscopy. Sensors (Basel) 2020;20:4256.

Cite this article as: Cong M, Li W, Liu Y, Bi J, Wang X, Yang X, Zhang Z, Zhang X, Zhao YN, Zhao R, Qiu J. Biomedical application of terahertz imaging technology: a narrative review. Quant Imaging Med Surg 2023;13(12):8768-8786. doi: 10.21037/qims-23-526

